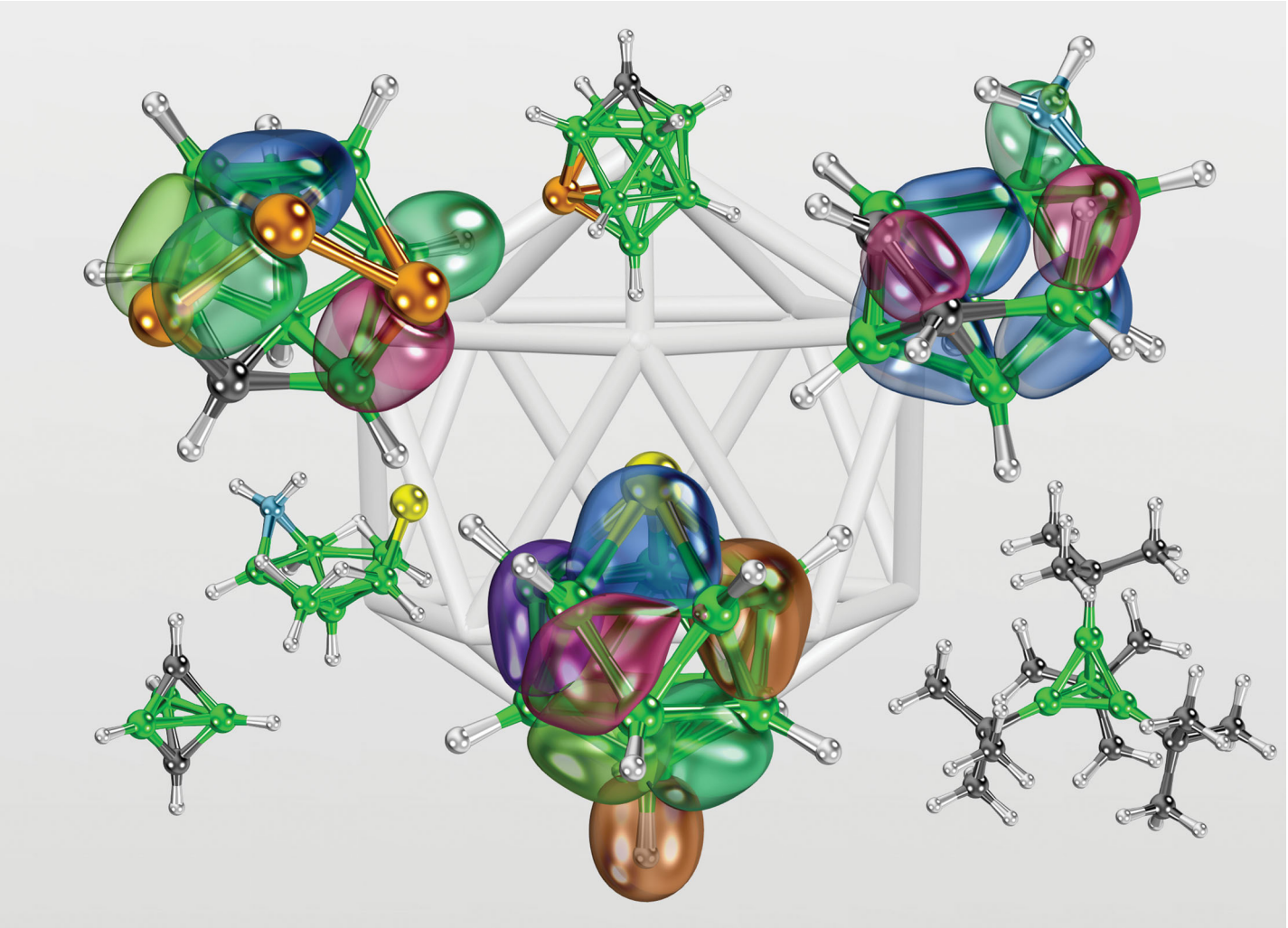

Showcasing research from the group of Dr Drahomír Hnyk at the Institute of Inorganic Chemistry of the Czech Academy of Sciences, Czech Republic.

A systematic examination of classical and multi-center bonding in heteroborane clusters

This paper presents a systematic study of multicenter and classical bonding on a broad series of various known heteroboranes with incorporated tetrel, pnictogen or chalcogen heterovertices up to the third-row elements. The nature of bonding is studied by a novel quantum-chemical tool, the intrinsic atomic/bond orbital (IAO/IBO) approach, which provides a direct connection between quantum chemistry and chemical concepts, the latter being exemplified by interatomic distances, molecular electrostatic potential surfaces and dipole moments.

As featured in:

See Drahomír Hnyk, Jindřich Fanfrlík *et al.*, *Phys. Chem. Chem. Phys.*, 2018, **20**, 4666.

ROYAL SOCIETY OF CHEMISTRY

rsc.li/pccp

Registered charity number: 207890

PCCP

PAPER

View Article Online
View Journal | View Issue

Cite this: *Phys. Chem. Chem. Phys.*, 2018, **20**, 4666

A systematic examination of classical and multi-center bonding in heteroborane clusters†

Petr Melichar,[a] Drahomír Hnyk *[b] and Jindřich Fanfrlík *[a]

Received 2nd November 2017,
Accepted 15th December 2017

DOI: 10.1039/c7cp07422k

rsc.li/pccp

This paper presents a systematic study of multicenter and classical bonding on a broad series of experimentally known heteroboranes covering *closo*, *nido*, *arachno* and *hypho* types of cages with incorporated tetrel, pnictogen or chalcogen heterovertices up to the third-row elements. The nature of bonding is studied using a novel quantum-chemical tool, the intrinsic atomic/bond orbital (IAO/IBO) approach, which provides a direct connection between quantum chemistry and chemical concepts. We also discuss how the computed IBO properties are related to molecular observables such as interatomic distances, molecular electrostatic potential surfaces and dipole moments.

Introduction

Bonding in boron clusters (boron hydrides, boranes) is predominantly of multicenter nature, and usually referred to as 3-center-2-electron (3c2e) bonding.[1–4] Two types of 3c2e bonds, B–B–B and B–H–B triangles, occur in boranes. The bridging B–H–B triangles of B_2H_6 led W. N. Lipscomb to formulate the concept of multicenter bonding. The Nobel Prize was awarded to him for the explanation of the differences between boranes and analogous organic compounds. The geometries of boranes and hydrocarbons are not compatible even in the case of simple B_2H_6 and C_2H_6 molecules. B_2H_6 with D_{2h} symmetry differs from the ethane structure with D_{3d} symmetry. Conceivably, B_2H_6 could be fitted to the electron diffraction data only when a hydrogen-bridge-based model of D_{2h} symmetry is considered.[5]

Multicenter bonding is not limited to boranes. It has been shown by using high-angle X-ray diffraction that the bonding in the trimethylaluminium dimer (Al_2Me_6) has multicenter character.[6] Multicenter bonding was also proposed for heteroborane clusters. W. N. Lipscomb *et al.* studied the nature of bonding in *closo*-carboranes at the semiempirical quantum mechanical level (the partial retention of diatomic differential overlap/PRDDO/method[7]).[8] In Lipscomb's classical view of 3c2e bonding, n atomic orbitals are combined into 3c2e bonds by forming only $n/3$ bonding orbitals. Extra electrons would have to occupy antibonding orbitals. A valence pattern for a given number of atoms is thus restricted to a few well-defined possibilities. Further attention has been paid to smaller cages such as *closo*-1,2-$Y_2B_3H_5$ (Y = CH, N, P), where it has been known that both 3c2e and 2c2e alternatives are possible.[9] Since the effort to study the bonding of heteroroboranes has focused mainly on smaller *closo*-carboranes, the knowledge of bonding in other heteroborane architectures is very limited.

Recently, it has also been possible to analyze bonding patterns using a novel quantum-chemical tool, the intrinsic atomic/bond orbital (IAO/IBO) method.[10] This method provides a direct connection between quantum chemistry and intuitive chemical concepts. It helps in determining the nature of chemical bonding from first principles calculations and computes the nature and shape of chemical bonds in terms of connecting quantitative SCF wave functions to a qualitative chemical picture (see Scheme 1).

Generally speaking, the bonding character illustrated (*e.g.* in the form of not assumed Lewis structures) thus naturally emerges. This procedure thus goes beyond the standard natural bond orbital (NBO) approach,[11a] which assumes a spherical symmetry of AOs and Lewis bonding patterns. Boldyrev has also

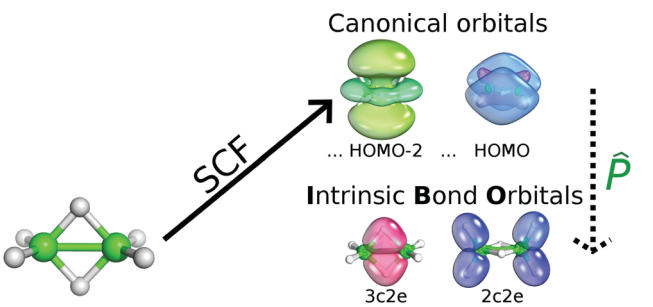

Scheme 1 Simplification of the intrinsic bond orbital (IBO) methodology.

[a] *Institute of Organic Chemistry and Biochemistry of the Czech Academy of Sciences, Flemingovo nam. 2, 166 10 Prague 6, Czech Republic. E-mail: fanfrlik@uochb.cas.cz*

[b] *Institute of Inorganic Chemistry of the Czech Academy of Sciences, v.v.i., 250 68 Husinec-Řež, Czech Republic. E-mail: hnyk@iic.cas.cz*

† Electronic supplementary information (ESI) available: The summarized IBO data for 7-, 9-, and 11-vertex *closo*-heteroboranes and the NBO results for selected representative boranes. See DOI: 10.1039/c7cp07422k

introduced a tool known as adaptive natural density partitioning (AdNP),[11b] a method that analyzes the first-order reduced density matrix, which inherently contains some assumptions. However, this approach works well for various boron rings such as boron molecular Wankel motors, boron fullerenes and 2D boron sheets.[11c] The wave function used for IBOs is initially calculated using canonical molecular orbitals (MOs) from the SCF procedure, and their subsequent unitary transformation yields the desired IBOs, which clarifies the nature of the corresponding bonding pattern. The point is that basis set functions are not associated with any atom. In the case of expanding MOs over a minimal basis set of free-atom AOs (known from any textbook of general chemistry), the resulting wave function can easily be interpreted. However, such a wave-function would be imprecise because the free-atom AOs do not undergo any polarization from the corresponding surroundings. On that basis, an accurate wave function is calculated and a set of polarized AOs is formed in terms of splitting the free-atom AOs into contributions corresponding to a depolarized occupied space and its complement by the corresponding projection.

We have applied the novel IBO approach to a broad series of experimentally known heteroboranes covering *closo*, *nido*, *arachno* and *hypho* types of cages with incorporated tetrel, pnictogen or chalcogen heterovertices up to the third-row elements in order to study the nature of bonding in heteroborane clusters.

Classical and multicenter bonding patterns are reflected in observable molecular properties. Firstly, the different bonding arrangements of various bonding types result in various interatomic distances that are slightly longer in multicenter bonds, as exemplified further. An interatomic distance close to the sum of the covalent radii (Σr_{cov})[1c] of both atoms can thus be considered as an indication of classical bonding. However, it might be questionable whether a larger interatomic distance necessarily indicates multicenter bonding. It might also be a consequence of electron deficiency in the case of electron unsaturated boranes. In this study, the obtained IBO results are compared with the interatomic distances refined either from the experimental electron diffraction or from the combined *ab initio*/GIAO/NMR approach. Secondly, classical bonding follows the established electronegativity concept, which is not true for multicenter bonding.[1b] We have thus computed and analyzed the molecular electrostatic potential (ESP) surfaces and the dipole moments of selected representative molecules.

Methods

In the first step, the IBO method was validated on a series of organic and inorganic compounds with well described either covalent or multicenter bonding: ethane, elemental white phosphorus P_4 and hydrogen disulfide (containing classical, 2c2e bonding), trimethylaluminium dimer,[6] diborane,[12] *closo*-$B_{12}H_{12}^{2-}$,[13] *nido*-$B_{11}H_{11}^{4-}$,[14] *arachno*-$B_{10}H_{14}^{2-}$,[15] *closo*-$B_{10}H_{10}^{2-}$,[13b] *closo*-$B_8H_8^{2-}$,[16] *closo*-$B_7H_7^{2-}$,[17] *closo*-$B_6H_6^{2-}$,[18] *closo*-$B_5H_5^{2-}$,[19] and tetra-*tert*-butyltetrabora-tetrahedrane.[20]

In the second step, we used the IBO method to investigate the nature of bonding in a series of experimentally known heteroboranes containing only up to third-row elements, specifically: *closo*-1-$CB_{11}H_{12}^-$,[21] *closo*-1,2-$C_2B_{10}H_{12}$,[22] *closo*-1,7-$C_2B_{10}H_{12}$,[22] *closo*-1-$NB_{11}H_{12}$,[23] *closo*-1,2-$P_2B_{10}H_{10}$,[24] *closo*-1,7-$P_2B_{10}H_{10}$,[25] *closo*-1-$SB_{11}H_{11}$,[26] *closo*-2-$CB_{10}H_{11}^-$,[27] *closo*-2,3-$C_2B_9H_{11}$,[28] *closo*-1-$CB_9H_{10}^-$,[29] *closo*-1,2-$C_2B_8H_{10}$,[30] *closo*-1,6-$C_2B_8H_{10}$,[31] *closo*-1,10-$C_2B_8H_{10}$,[32] *closo*-1-NB_9H_{10},[33] *closo*-2,1-PCB_8H_9,[34] *closo*-6,1-PCB_8H_9,[34] *closo*-1-SB_9H_9,[35] *closo*-4-$CB_8H_9^-$,[36] *closo*-1,7-$C_2B_7H_9$,[37] *closo*-1-$CB_7H_8^-$,[38] *closo*-1,2-$C_2B_6H_8$,[39] *closo*-1,7-$C_2B_6H_8$,[40] *closo*-1,6-$C_2B_6H_8$,[39] *closo*-2-$CB_6H_7^-$,[41] *closo*-2,4-$C_2B_5H_7$,[42] *closo*-1,2-$C_2B_4H_6$,[43] *closo*-1,6-$C_2B_4H_6$,[42] *closo*-1,5-$C_2B_3H_5$,[42] *closo*-2,3-$C_2B_3H_5$,[42] *closo*-1,2-$C_2B_3H_5$,[42] *nido*-2,9-$C_2B_9H_{12}^-$,[44] *nido*-2,7-$C_2B_9H_{12}^-$,[45] *nido*-7,8-$C_2B_9H_{12}^-$,[46] *nido*-7,9-$C_2B_9H_{12}^-$,[44] *nido*-7,8,10-$C_2SB_8H_{10}$,[47] *nido*-9,11,7,8-$P_2C_2B_7H_9$,[48] *nido*-7,8,9,10-$P_2C_2B_7H_9$,[48] *nido*-7,8,9,10-$P_3CB_7H_8$,[49] *nido*-7,9,8,10-$P_2C_2B_7H_9$,[48] *nido*-7,8,9,11-$P_2C_2B_7H_9$,[48] *nido*-6,7-$C_2B_7H_9^{2-}$,[49] *arachno*-1,8,11-$NC_2B_8H_{13}$,[50] *arachno*-6,9-CSB_8H_{12},[51] *arachno*-4,6,5-$C_2SB_6H_{10}$,[52] *hypho*-2,5,12-$C_3B_8H_{15}^-$,[53] *hypho*-7,8-$C_2B_6H_{13}^-$,[54] *hypho*-7,8-NSB_6H_{11},[54] *hypho*-7,8-$S_2B_6H_9^-$,[54] and *hypho*-7,8-$CSB_6H_{11}^-$.[54] Because of the *hypho* *vs.* *nido* conflict present, the classification of such compounds as *hypho* should be treated with caution.[54] The numbering of the studied cages is shown in Fig. 1.

All the calculations were performed at the DFT/B3-LYP/def2-TZVPP level of theory using the Turbomole6.6[55] and Gaussian09[56] program packages. The outputs were examined using the IBOview program[10] to visualize the IBOs (threshold of 60%) and render it. Furthermore, the electrostatic potential and the dipole moments were computed at the HF/cc-pVDZ level using the Gaussian09[56] and Molekel4.3[57] program packages.

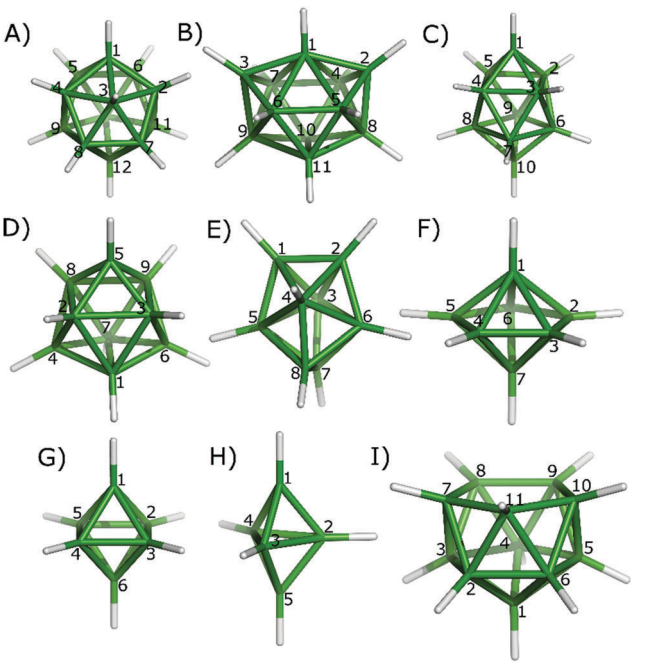

Fig. 1 The numbering scheme for the following studied cages: *closo*-$B_{12}H_{12}^{2-}$ (A), *closo*-$B_{11}H_{11}^{2-}$ (B), *closo*-$B_{10}H_{10}^{2-}$ (C), *closo*-$B_9H_9^{2-}$ (D), *closo*-$B_8H_8^{2-}$ (E), *closo*-$B_7H_7^{2-}$ (F), *closo*-$B_6H_6^{2-}$ (G), *closo*-$B_5H_5^{2-}$ (H) and *nido*-$B_{11}H_{11}^{4-}$ (I).

Results and discussion

Benchmarks

To validate the IBOs and illustrate the difference between the 2c2e and 3c2e types of bonding, we first applied the IBO approach to a series of organic/inorganic compounds with 2c2e bonding and *closo*-borane clusters with 3c2e bonding. In addition, we considered the bridging Al–C bonds in $Al_2(CH_3)_6$ because the multicenter bonding of this molecule had been confirmed experimentally.[6]

The IBOs for the benchmark organic/inorganic compounds and the selected boron clusters are summarized in Fig. 2. The IBOs clearly demonstrated classical bonding in ethane, elemental white tetraphosphorus P_4 and disulfide hydrogen (Fig. 2A–C). The IBOs also confirmed multicenter bonding in $Al_2(CH_3)_6$ (Fig. 2D) in accordance with the experimental data. In addition, the hydrogen bridging in diborane was also shown to be of multicenter nature (Fig. 2E). The interatomic distances are slightly elongated in the shown multicenter bonds. The B–H, B–B and C–Al separations are 4–14% longer than the sum of the covalent radii (Σr_{cov})[1c] of both atoms, *i.e.* distances of 1.334, 1.770[5] and 2.125[6] Å, respectively. For comparison, the classical 2c2e B–H and C–Al bonds of the same molecules are closer to Σr_{cov}, *i.e.* 1.187[5] and 1.953[6] Å, which correspond to 101.5 and 97.2% of Σr_{cov}, respectively. In addition, the terminal (exosceletal) H atoms involved in the classical 2c2e B–H bonds have hydridic character due to the low electronegativity of B atoms. In contrast to the terminal H atoms, the bridging H atoms of diborane have partial positive atomic charges.[58]

In the series of various borane clusters, the presence of multicenter bonding was confirmed (Fig. 2F and G). Besides the 3c2e bonds, this approach also revealed 4-center-2-electron (4c2e)[59] bonds of the B–B–B–B type in *closo*-$B_nH_n^{2-}$ (n = 12, 10 and 8), *nido*-$B_{11}H_{11}^{4-}$ and *arachno*-$B_{10}H_{14}^{2-}$. This unique 4c2e bonding has already been known for some borane compounds.[60,61] However, this bonding has only been reported as 4c2e B–B–B–H with no evidence for 4c2e B–B–B–B bonding. The presence of the 4c2e bond in *closo*-$B_{12}H_{12}^{2-}$ is shown in Fig. 2F. The number of 4c2e bonds increased with the size of the cluster (*e.g.* *closo*-$B_{10}H_{10}^{2-}$ and *closo*-$B_{12}H_{12}^{2-}$ had one and three 4c2e bonds, respectively).

In the case of tetra-*tert*-butyl-tetrabora-tetrahedrane, $B_4(t\text{-Bu})_4$ (see Fig. 2H), the IBO approach clearly indicated the presence of four multicenter 3c2e bonds (B–B–B triangles). The other bonds, including the B–C, C–C and C–H bonds, were confirmed by the IBOs to be of classical 2c2e nature. The observed presence of 3c2e bonding corresponded well with the published study on B_4H_4 and $B_4(CH_3)_4$.[62]

Bonding in heteroboranes

It is important to consider the differences between various boron architectures when analyzing the results for multidimensional boron compounds – *e.g.* *closo*-1-$SB_{11}H_{11}$ differs in many respects from *closo*-1-SB_9H_9.[63] The IBO results of icosahedral heteroboranes are summarized in Table 1. Furthermore, the IBOs of selected *closo*-heteroborane clusters are shown in Fig. 3. When the icosahedral

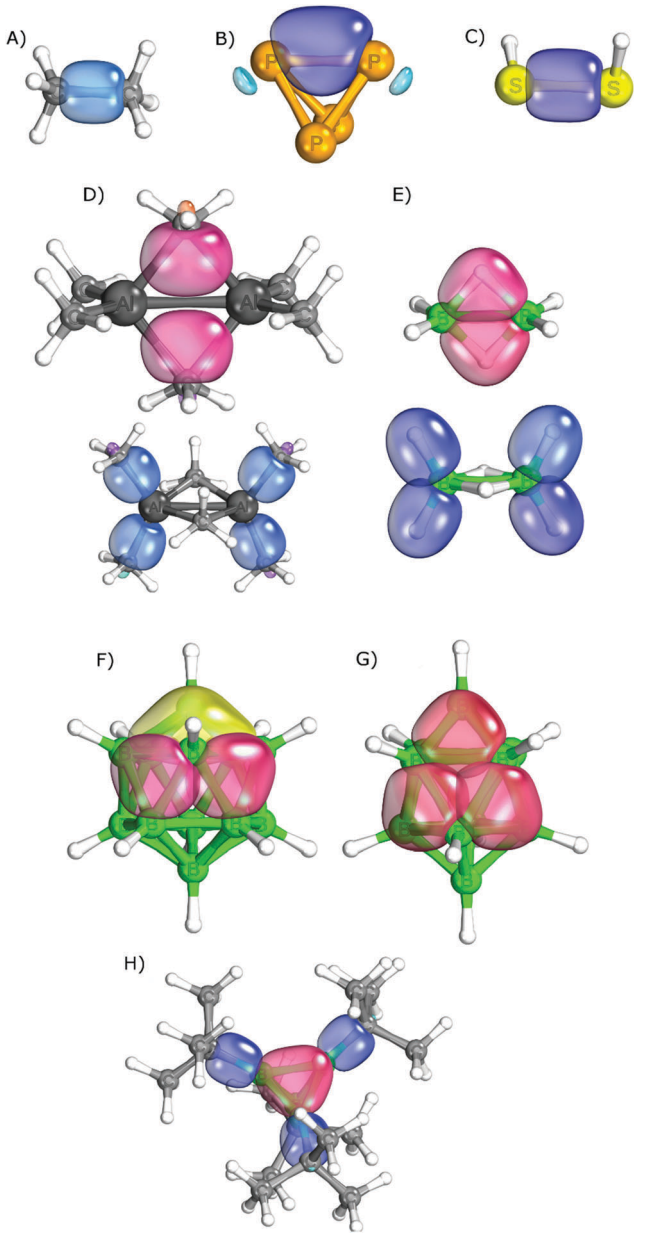

Fig. 2 The visualized IBOs for selected organic/inorganic compounds (A–C), trimethylaluminium (D), diborane (E) *closo*-$B_{12}H_{12}$ (F), *closo*-$B_{10}H_{10}$ (G) and tetra-*tert*-butyl-tetrabora-tetrahedrane (H). The orbital color coding is as follows: dark blue/purple – classical 2c2e bonding; red/pink – multicenter 3c2e bonding; yellow – multicenter 4c2e bonding.

cluster only contained a single heteroatom, the heteroatom was mostly part of multicenter bonding. For instance, the C atom of *closo*-1-$CB_{11}H_{12}^-$ participated in three bonds, one of 4c2e nature (B–B–B–C) and two of 3c2e nature (B–B–C, see Fig. 3A). This bonding was thus analogous to the parent *closo*-$B_{12}H_{12}^{2-}$, which also contained one 4c2e and two 3c2e bonds in the same location. Similarly, the S atom of *closo*-1-$SB_{11}H_{11}$ (see Fig. 3B) took part in two multicenter (3c2e) bonds of B–S–B type and one bond of B–B–S–B type of 4c2e nature. Such a bonding pattern corresponded to a B–S distance of 2.010 Å (106.9% of Σr_{cov}).[26a] More interestingly, it could also help in explaining the highly

Table 1 The summarized IBO data for the icosahedral heteroboranes. For the sake of clarity, the B–B–H and B–B–B multicenter bonds are not included

	Bonding	
Compound	Multicenter	Classical
12-vertex		
closo-1-$CB_{11}H_{12}^-$	2 × B–C–B; 1 × B–C–B–B	—
closo-1-$SB_{11}H_{11}$	1× B–S–B; 1 × B–S–B–B	—
closo-1-$NB_{11}H_{12}$	2 × B–N–B	1 × B–N
closo-1,7-$C_2B_{10}H_{12}$	6 × B–C–B	—
closo-1,7-$P_2B_{10}H_{10}$	3 × B–P–B; 3 × B–B–P–B	—
closo-1,2-$C_2B_{10}H_{12}$	4 × B–C–B	1 × C–C
closo-1,2-$P_2B_{10}H_{10}$	4 × B–P–B; 1 × B–P–P–B	—

positive σ-holes ($V_{S,max}$ of 28.2 kcal mol^{-1}) on the S atom, which are known to be important for its crystal packing.[64] This $V_{S,max}$ value is unusually high considering the low electronegativity of boron atoms. *closo*-1-$NB_{11}H_{12}$ contained two 3c2e B–N–B bonds and one 2c2e B–N bond. However, it should be mentioned that the 2c2e bonding was debatable in the case of *closo*-1-$NB_{11}H_{12}$ (see Fig. 3C). The bond evaluated as a classical covalent bond was less localized than a typical 2c2e bond (Fig. 2) and could also be seen as a crossing between the 2c2e and 4c2e bonds. Such a bonding pattern would also better correspond to a B–N distance of 1.716 Å (110.0% of Σr_{cov}).[23]

closo-1,7-$C_2B_{10}H_{12}$ and *closo*-1,7-$P_2B_{10}H_{10}$ have two heteroatoms that are not adjacent. They can thus be considered as a crossing between heteroboranes with one and more heterovertices. In contrast to *closo*-1-$CB_{11}H_{12}^-$, the C atoms of *closo*-1,7-$C_2B_{10}H_{12}$ did not form 4c2e B–C–B–B bonds. Instead, they only formed B–C–B 3c2e multicenter bonds. *closo*-1,7-$P_2B_{10}H_{10}$, however, formed both 3c2e and 4c2e bonds. *closo*-1,2-$C_2B_{10}H_{12}$ has two adjacent C atoms, which form 3c2e B–C–B bonds and a classical C–C bond (see Fig. 3D). This pair of adjacent C–C atoms is known to act as an electron donor and becomes the center of the partial positive charge in the molecule. This has

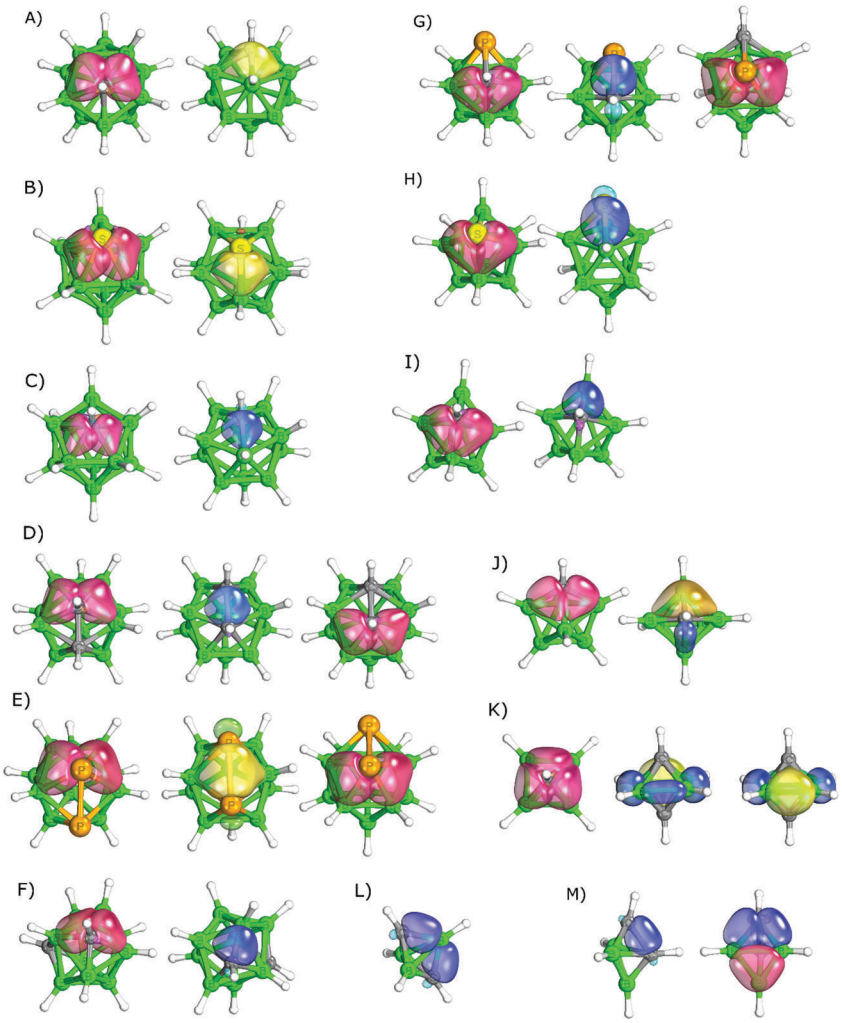

Fig. 3 Calculated IBOs for the following heteroboranes: *closo*-1-$CB_{11}H_{12}^-$ (A), *closo*-1-$SB_{11}H_{11}$ (B), *closo*-1-$NB_{11}H_{12}$ (C), *closo*-1,2-$C_2B_{10}H_{12}$ (D), *closo*-1,2-$P_2B_{10}H_{10}$ (E), *closo*-2,3-$C_2B_9H_{11}$ (F), *closo*-2,1-PCB_8H_9 (G), *closo*-1-SB_9H_9 (H), *closo*-1-$CB_7H_8^-$ (I), *closo*-2-$CB_6H_7^-$ (J), *closo*-1,6-$C_2B_4H_6$ (K), *closo*-1,5-$C_2B_3H_5$ (L) and *closo*-1,2-$C_2B_3H_5$ (M). The orbitals that are not shown in this figure are analogous to those rendered. The orbital color coding is as follows: dark blue/purple – classical 2c2e bonding; red/pink – multicenter 3c2e bonding; yellow – multicenter 4c2e bonding.

already been determined experimentally.[65] It might thus be considered important experimental evidence supporting the 3c2e B–C–B bonding. The C–C bond of *closo*-1,2-$C_2B_{10}H_{12}$ was the only classical bond found by the IBO approach among the icosahedral heteroboranes besides the debatable case of *closo*-1-$NB_{11}H_{12}$ described above. Similar to the B–N bond of *closo*-1-$NB_{11}H_{12}$, the C–C bond of *closo*-1,2-$C_2B_{10}H_{12}$ was less localized and longer (1.624 Å) than the C–C classical bonds in the validation data set, *e.g.* in ethane (1.540 Å).[22] It also corresponds to LMO results obtained by Lipscomb *et al.*[66] The studied icosahedral cluster with adjacent P atoms, *closo*-1,2-$P_2B_{10}H_{10}$ (see Fig. 3E), did not form a classical bond between the P atoms; instead, it formed a multicenter B–P–P–B 4c2e bond. This bonding could be compared to B–B–B–B obtained in the parent *closo*-$B_{12}H_{12}^{2-}$. The P–P distance in *closo*-1,2-$P_2B_{10}H_{10}$ is 2.310 Å (104.1% of Σr_{cov}).[24] The most positive molecular ESP surface is located between the two P atoms ($V_{S,max}$ = 28.2 kcal mol^{-1}),[67] which is analogous to *closo*-1,2-$C_2B_{10}H_{12}$.

The bonding patterns of the 11-vertex *closo*-carboranes were similar to those of the 12-vertex cages (compare Table 1 and Table S1, ESI†). The IBO results did not reveal any difference in bonding between *closo*-2-$CB_{10}H_{11}^-$ and the above-discussed *closo*-1-$CB_{11}H_{12}^-$. However, some difference was found between *closo*-2,3-$C_2B_9H_{11}$ and *closo*-1,7-$C_2B_{10}H_{12}$ (separated C atoms in both clusters, numbering shown in Fig. 1). The C atoms of *closo*-2,3-$C_2B_9H_{11}$ (see Fig. 3F) participated in a classical B–C bond besides the two B–C–B 3c2e bonds. On the other hand, *closo*-1,7-$C_2B_{10}H_{12}$ only had 3c2e B–C–B bonds.

The bonding patterns obtained in the 10-vertex *closo*-heteroboranes (see Table 2) were also overall similar to those in the icosahedral cages. *closo*-1-$CB_9H_{10}^-$ and *closo*-1,2-$C_2B_8H_{10}$ had analogous bonding patterns to *closo*-1-$CB_{11}H_{12}^-$ and *closo*-1,2-$C_2B_{10}H_{12}$, respectively. It should be mentioned, however, that the C–C bond of *closo*-1,2-$C_2B_8H_{10}$ is shorter than that bond in *closo*-1,2-$C_2B_{10}H_{12}$, (1.538 *vs.* 1.624 Å).[30] In addition, the bonding in *closo*-2,1-PCB_8H_9 (see Fig. 3G) was similar to *closo*-1,2-$C_2B_{10}H_{12}$. Besides *closo*-1,2-$C_2B_8H_{10}$, two other isomers of *closo*-$C_2B_{10}H_{12}$ were studied, both with non-adjacent C atoms.

Table 2 The summarized IBO data for various *closo*-heteroboranes. For the sake of clarity, B–B–H and B–B–B multicenter bonds are not included

	Bonding	
Compound	Multicenter	Classical
10-vertex		
closo-1-$CB_9H_{10}^-$	2 × B–C–B; 1 × B–C–B–B	—
closo-1,2-$C_2B_8H_{10}$	4 × B–C–B	1 × C–C
closo-1,6-$C_2B_8H_{10}$	5 × B–C–B; 1 × B–C–B–B	—
closo-1,10-$C_2B_8H_{10}$	5 × B–C–B; 1 × B–C–B–B	—
closo-1-NB_9H_{10}	2 × B–N–B	1 × B–N
closo-2,1-PCB_8H_9	2 × B–P–B; 2 × B–C–B	1 × C–P
closo-6,1-PCB_8H_9	3 × B–C–B; 2 × B–P–B; 1 × B–P–B–B	—
closo-1-SB_9H_9	2 × B–S–B	1 × B–S
8-vertex		
closo-1-$CB_7H_8^-$	2 × B–C–B	1 × B–C
closo-1,2-$C_2B_6H_8$	4 × B–C–B	1 × C–C
closo-1,7-$C_2B_6H_8$	4 × B–C–B; 2 × B–C–B–B	—
closo-1,6-$C_2B_6H_8$	4 × B–C–B; 2 × B–C–B–B	—

Both clusters only formed multicenter bonds of either 3c2e or 4c2e nature. The fact that these molecules formed a 4c2e bond corresponded to the parent *closo*-$B_{10}H_{10}^{2-}$, in which a 4c2e bond occurred as well. The analysis of *closo*-1-NB_9H_{10} revealed very similar results to the above-discussed *closo*-1-$NB_{11}H_{12}$. Both of these molecules had a single 2c2e B–N bond. This might be in accordance with *closo*-1-SB_9H_9, where two multicenter B–S–B bonds and one classical B–S bond were found. When *closo*-1-SB_9H_9 (see Fig. 3H) was compared to *closo*-1-$SB_{11}H_{11}$, one classical B–S bond was formed instead of a B–S–B–B 4c2e bond. This finding might help to rationalize the less positive σ-holes (22.4 *vs.* 28.2 kcal mol^{-1})[67] and the shorter S–B distance (1.939[35a] *vs.* 2.010[26a] Å) in *closo*-1-SB_9H_9.

Two *closo*-carborane cages with 9 vertices were considered (Table S1, ESI†): *closo*-4-$CB_8H_9^-$ and *closo*-1,7-$C_2B_7H_9$. Only B–C–B 3c2e bonds were found in these molecules. The absence of 4c2e bonding in *closo*-4-$CB_8H_9^-$ could be caused by differences in the architecture of the cage. Otherwise, the data were in agreement with the results obtained for the larger *closo*-cages, discussed above.

The bonding patterns observed across the 8- and 7-vertex *closo*-carbaboranes were overall similar to the bigger ones (see Tables 1 and 2). However, one significant difference was found. While the IBOs did not show any C–B classical bonding in the bigger *closo*-$CB_{n-1}H_n^-$ (n = 9–12) cages, the C atom of *closo*-$CB_{n-1}H_n^-$ (n = 7–8) formed a classical 2c2e B–C bond as well as multicenter bonds.

The 6- and 5-vertex *closo*-dicarbaboranes showed different trends from the bigger ones. Classical bonding was still more frequent in the smallest cages. In addition to the C–C and B–C bonds, the classical B–B bond was also found in *closo*-1,6-$C_2B_4H_6$ and *closo*-2,3-$C_2B_3H_5$ (see Table 3 and Fig. 3). Furthermore, the IBOs even disproved the presence of any multicenter bonding in *closo*-1,5-$C_2B_3H_5$. All bonds appeared to be B–C classical bonds. Such a bonding pattern would correspond to the localized molecular orbital (LMO) structures,[8] which were already used to question the presence of the multicenter nature of the C–B–C bonding in *closo*-1,5-$C_2B_3H_5$.[68] Note that the small cluster dimensions are problematic cases in terms of ^{11}B NMR computations.[20b] In addition, the interatomic distances and charge distribution should reflect the classical bonding pattern. The short C–B separation (1.553 Å,[20b] 97.1% of Σr_{cov}) supports the classical bonding pattern. It should also be mentioned that

Table 3 The summarized IBO data for various *closo*-heteroboranes. For the sake of clarity, B–B–H and B–B–B multicenter bonds are not included

	Bonding	
Compound	Multicenter	Classical
6-vertex		
closo-1,2-$C_2B_4H_6$	4 × B–C–B	1 × C–C
closo-1,6-$C_2B_4H_6$	6 × B–C–B; 1 × C–B–B–C	3 × B–B
5-vertex		
closo-1,5-$C_2B_3H_5$	—	6 × B–C
closo-2,3-$C_2B_3H_5$	2 × B–C–B; 1 × B–C–C–B	2 × B–C; 2 × B–B
closo-1,2-$C_2B_3H_5$	2 × B–C–B	1 × C–C; 2 × B–C

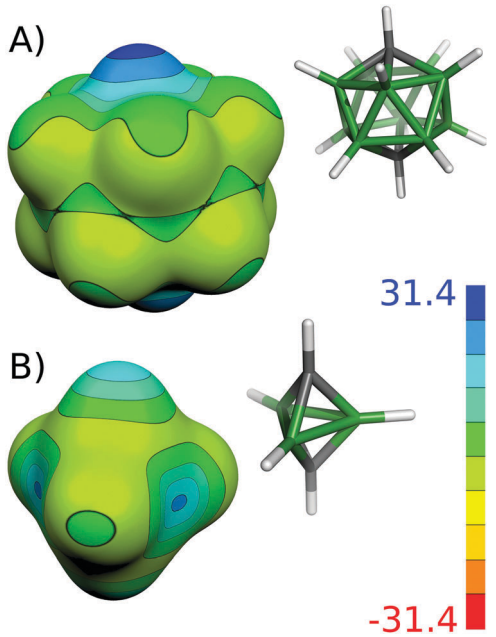

Fig. 4 The molecular diagrams and electrostatic potential on the 0.001 a.u. molecular surface for *closo*-1,12-$C_2B_{10}H_{11}$ (A) and *closo*-1,5-$C_2B_3H_5$ (B). The color range of the ESP is in kcal mol^{-1}.

the B–B separation in these molecules is 1.844 Å[20b] (108.5% of Σr_{cov}) and the IBO did not show any bonding between these boron atoms. In contrast to the other *closo* carboranes, the most positive ESP of *closo*-1,5-$C_2B_3H_5$ is not on the top of the CH vertex; instead, it is on the B atom (see Fig. 4). This finding shows that the classical electronegativity concept is valid in this molecule, which supports classical bonding in this molecule.

The IBO results of *closo*-1,2-$C_2B_4H_6$ did not differ from the IBO results of the bigger *closo*-1,2-$C_2B_{n-2}H_n$ (n = 12, 10, 8), in contrast to the other smaller compounds. The C atom participated in four B–C–B bonds and one C–C bond in all of these *closo*-1,2-$C_2B_{n-2}H_n$ (n = 12, 10, 8, 6) molecules. The IBO results of *closo*-1,2-$C_2B_4H_6$ nicely resembled the LMO structures on the PRDDO level obtained using the Boys criteria.[8]

The bonding results for *nido*- are summarized in Table 4. The calculated IBOs for the selected heteroborane clusters are included in Fig. 5 to illustrate their bonding. The results show that the nature of bonding is heavily dependent on the position of the heteroatom in the *nido*-cages. Covalent bonds were found exclusively in the open face. For example, *nido*-2,9-$C_2B_9H_{12}$ and *nido*-2,7-$C_2B_9H_{12}$, which had one C atom located in the open face and one in the closed face, only formed the classical B–C bonds on the open belt, whereas the carbon in the closed face only participated in bonding of 3c2e nature. Moreover, although *nido*-2,7-$C_2B_9H_{12}$ had adjacent carbon atoms, the classical C–C bonding did not occur. Instead, C–C–B bonding of 3c2e nature was formed. On the other hand, when a *nido*-cage contained at least one heteroatom in the open pentagonal belt, evidence for classical covalent bonding was found. *nido*-Carboranes with two C atoms in the face formed B–C–B, B–C and C–C bonds. *nido*-7,8-$C_2B_9H_{12}$ contained adjacent C atoms and thus formed one C–C and two B–C bonds of classical 2c2e nature. *nido*-7,9-$C_2B_9H_{12}$ with separated C atoms formed four B–C bonds of 2c2e nature, all in the open face. The 3c2e bonds were formed in B–C–B triangles, when both B atoms were located under the C atom.

The bonding patterns of the *nido*-cages with other incorporated heteroatoms were very similar to the already-described *nido*-carboranes. Any heteroatom incorporated into the open face

Table 4 The summarized IBO data for various *nido*-, *arachno*- and *hypho*-heteroboranes. For the sake of clarity, the multicenter B–B–H and B–B–B bonds are not included

	Bonding	
Compound	Multicenter	Classical
nido-		
nido-2,9-$C_2B_9H_{12}^-$	4 × B–C–B	2 × B–C
nido-2,7-$C_2B_9H_{12}^-$	1 × B–C–C; 2 × B–C–B	2 × B–C
nido-7,8-$C_2B_9H_{12}^-$	2 × B–C–B	1 × C–C; 2 × B–C
nido-7,9-$C_2B_9H_{12}^-$	2 × B–C–B	4 × B–C
nido-7,8,10-$C_2SB_8H_{10}$	1 × B–S–B	2 × B–S; 2 × B–C; 1 × C–C
nido-9,11,7,8-$P_2C_2B_7H_9$	2 × B–C–B; 2 × B–P–B	2 × B–P; 2 × C–P; 1 × C–C
nido-8,9,7,11-$P_2C_2B_7H_9$	2 × B–P–B; 2 × B–C–B	1 × P–P; 1 × C–C; 1 × C–P; 1 × B–C; 1 × P–B
nido-7,8,9,10-$P_3CB_7H_8$	3 × B–P–B; 1 × B–C–B	2 × P–P; 1 × P–C; 1 × B–C; 1 × B–P
nido-7,9,8,10-$P_2C_2B_7H_9$	2 × B–P–B; 2 × B–C–B	3 × P–C; 1 × B–P; 1 × B–C
nido-7,8,9,11-$P_2C_2B_7H_9$	2 × B–P–B; 2 × B–C–B	1 × P–P; 2 × P–C; 2 × B–C
nido-6,7-$C_2B_7H_9^{2-}$	2 × B–C–B	1 × C–C; 2 × B–C
arachno-		
arachno-1,8,11-$NC_2B_8H_{13}$	3 × B–C–B	1 × C–C; 2 × N–B
arachno-6,9-CSB_8H_{12}	2 × B–C–B	2 × B–S
arachno-4,6,5-$C_2SB_6H_{10}$	4 × B–C–B	2 × B–S
hypho-		
hypho-$C_3B_8H_{15}^-$	4 × B–C–B	2 × B–C
hypho-7,8-$C_2B_6H_{13}^-$	—	4 × B–C
hypho-7,8-NSB_6H_{11}	—	2 × B–S; 2 × N–B
hypho-7,8-$S_2B_6H_9^-$	—	4 × S–B
hypho-7,8-$SCB_6H_{11}^-$	—	2 × B–S; 2 × B–C

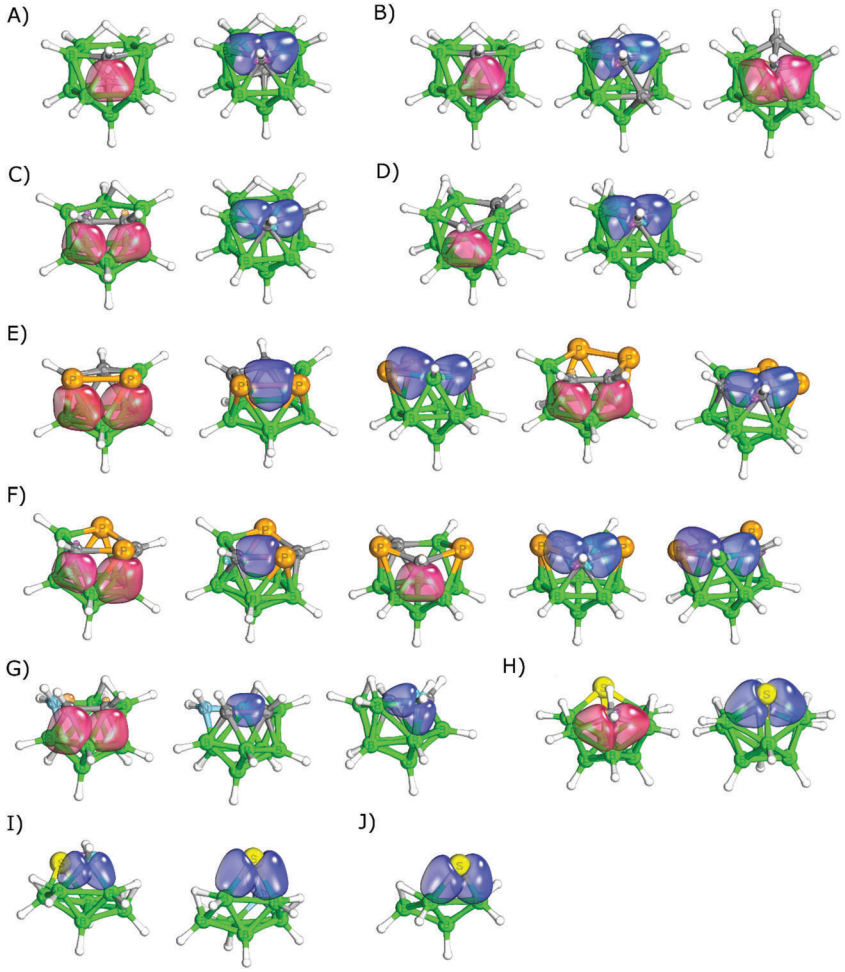

Fig. 5 Calculated IBOs for the following heteroboranes: *nido*-2,9-$C_2B_9H_{12}^-$ (A), *nido*-2,7-$C_2B_9H_{12}^-$ (B), *nido*-7,8-$C_2B_9H_{12}^-$ (C), *nido*-7,9-$C_2B_9H_{12}^-$ (D), *nido*-7,8,9,10-$P_2C_2B_7H_9$ (E), *nido*-7,9,8,10-$P_2C_2B_7H_9$ (F), *arachno*-1,8,11-$NC_2B_8H_{13}$ (G), *arachno*-6,9-CSB_8H_{12} (H), *hypho*-7,8-NSB_6H_{11} (I) and *hypho*-7,8-$S_2B_6H_9^-$ (J). The orbitals that are not shown in this figure are analogous to those rendered. The orbital color coding is as follows: dark blue/purple – classical 2c2e bonding; red/pink – multicenter 3c2e bonding; yellow – multicenter 4c2e bonding.

was a source of classical bonding. This resulted in a variety of bonding. For example, the open belts of *nido*-7,8,10-$C_2SB_8H_{10}$, *nido*-7,8,9,10-$P_3CB_7H_8$, *nido*-7,8,9,10-$P_2C_2B_7H_9$ and *nido*-9,11,7,8-$P_2C_2B_7H_9$ were formed exclusively *via* the classical covalent bonds. There was evidence for S–B, P–P, C–C, C–P, B–C and P–B classical bonds. The length of these bonds ranged from 98.3 to 102.0% of Σr_{cov}, thus supporting the classical bonding pattern.[47–49] Besides the classical bonds in the open face, the *nido*-heteroboranes also contained multicenter bonds of 3c2e nature with the participating heteroatom in agreement with the above-described *nido*-carboranes. In *nido*-8,9,7,11-$P_2C_2B_7H_9$, the 3c2e B–P–B bonds were formed in the triangles 3–4–8 and 4–5–9 (the numbering of this cage is shown in Fig. 1I). Similarly, B–C–B 3c2e bonds were formed in the 2–6–11 and 2–3–7 triangles. The interatomic distances ranged from 103.9 to 108.7% of Σr_{cov} in these triangles.[48] *nido*-9,11,7,8-$P_2C_2B_7H_9$ had an analogous bonding pattern even though the P atoms were not adjacent.

When the two heteroatoms were adjacent to each other, two 3c2e bonds of B–Z–B (Z = various heteroatoms) were formed. Here, one boron atom was shared by both of the triangles. This one lay on the under-belt under the middle of the Z–Z covalent bonding. When the heteroatoms were not located adjacent to each other, the 3c-2e triangles were still formed. The heteroatoms and boron atoms lying under them are involved in this kind of bonding. The computed dipole moments and molecular ESP surfaces of the representative *nido* clusters show that the heterovertices located in the open pentagonal face act as an electron donor and become the center of a partial positive charge of the molecule (Fig. 6), which supports the existence of the B–Z–B 3c2e bonds. Moreover, the crystal packing of *nido*-7,8,9,11-$Sb_2C_2B_7H_9$ is predominantly dictated by the very strong $Sb_2\cdots H$–B σ-hole interaction.[48b]

We also applied the IAO method to *nido*-6,7-$C_2B_7H_9$ as a representative of the 9-vertex *nido*-heteroboranes. Two B–C–B bonds of 3c2e nature and B–C and C–C 2c2e bonds suggested that bonding in the 9-vertex is not different from the 11-vertex *nido*-clusters.

The IBO results of the *arachno*-clusters are summarized in Table 4 and some of them have also been selected for Fig. 5, where the IBO results are illustrated. The results were similar to

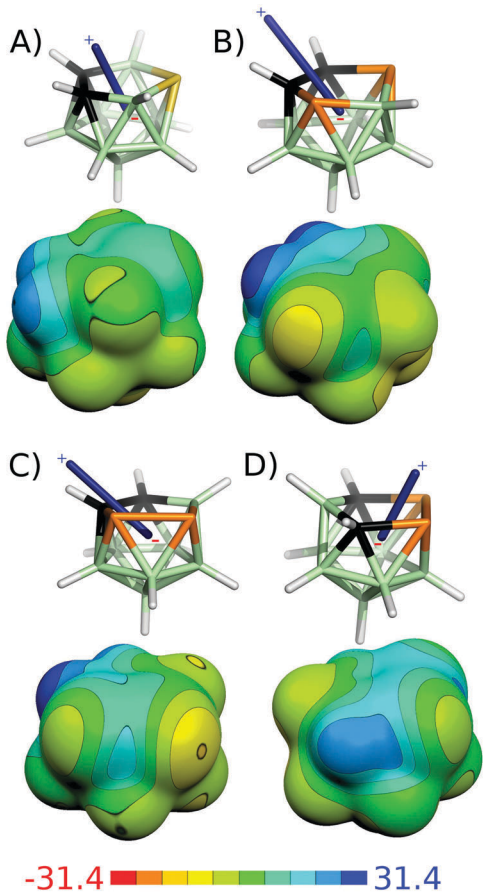

Fig. 6 The visualization of the calculated dipole moment and electrostatic potential (ESP) on the 0.001 a.u. molecular surface of *nido*-7,8,10-$C_2SB_8H_{10}$ (A), *nido*-9,11,7,8-$P_2C_2B_7H_9$ (B), *nido*-8,9,7,11-$P_2C_2B_7H_9$ (C) and *nido*-7,8,9,11-$P_2C_2B_7H_9$ (D). The color range of the ESP is in kcal mol^{-1}.

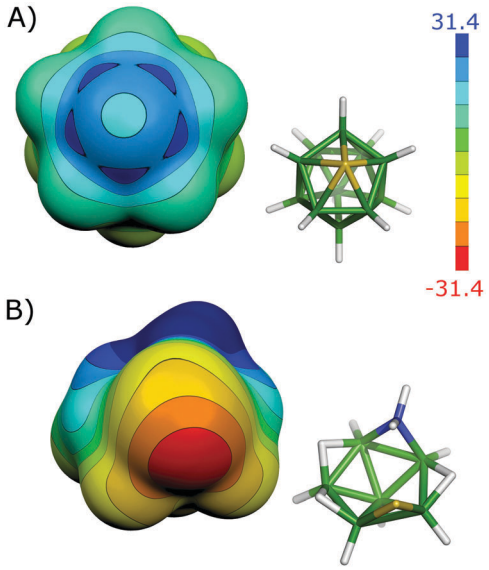

Fig. 7 The molecular diagrams and electrostatic potential on the 0.001 a.u. molecular surface of *closo*-1-$SB_{11}H_{11}$ (A) and *hypho*-7,8-NSB_6H_{11} (B). The color range of the ESP is in kcal mol^{-1}.

those of the *nido*-clusters. The C atoms were bonded *via* 3c2e B–C–B bonds in the *arachno*-clusters. In the case of *arachno*-1,8,11-$NC_2B_8H_{13}$ with adjacent carbon atoms, the classical C–C bond was formed. At the same time, two B–C–B multicenter bonds were formed as well (see Fig. 5G). The other heteroatoms only formed classical bonds, *e.g.* the S atom of *arachno*-4,6,5-$C_2SB_6H_{10}$ or the N atom of *arachno*-1,8,11-$NC_2B_8H_{13}$.

The calculated IBOs for *hypho*-clusters are summarized in Table 4. Their IBOs are shown in Fig. 5. Bonding of the heteroatoms was dominated by classical bonding in the studied *hypho*-clusters. With the exception of *hypho*-$C_3B_8H_{15}$, the IBOs did not reveal any bonds of multicenter nature with the exception of the B–B–B and B–B–H bonds. Each of the heteroatoms formed two covalent bonds with a boron atom of 2c2e nature.

In contrast to *closo*-1-$SB_{11}H_{11}$, the S atom of *hypho*-7,8-NSB_6H_{11} is incorporated into the *hypho*-cluster network exclusively *via* classical B–S bonds and consequently acts as an electron acceptor. This S atom thus has a negative electrostatic potential (ESP) surface without areas of positive ESP (see Fig. 7).

Table S2 (ESI†) shows the results for a selected series of representative compounds obtained by the most widely used orbital localization scheme, the NBO methodology. The NBO and IBO results are overall similar with many small differences. The majority of the differences are due to the different localization techniques used. While IBO only minimizes the spread of bond orbitals over the atoms (*i.e.* maximizes their localization), the NBOs explicitly search for the predefined Lewis structures most closely matching the given wave function. Consequently, 4c2e bonds naturally emerged in the IBO analysis of many heteroborane clusters. On the other hand, the NBO analysis was limited to 2c2e and 3c2e bonds. Other nonsystematic differences could be found between the IBO and NBO methods. However, an exhaustive comparison of the IBO with other methods is beyond the scope of this study.

Conclusions

The nature of bonding has been systematically studied on a broad series of heteroboranes using a novel quantum chemical tool, the intrinsic bond orbital (IBO) approach. The results have shown that the bonding of heteroatoms in icosahedral clusters is mainly of multicenter nature. The role of classical bonding increases with the decreasing size of the *closo*-heteroborane cages. An extreme case is *closo*-1,5-$C_2B_3H_5$, where the IBOs have disproved the presence of any multicenter bonding. The nature of bonding in the *nido*- and *arachno*-cages heavily depends on the position of the heteroatom, and covalent bonds have been found exclusively in the open face in *nido*- and *arachno*-cages. However, classical bonds are more common in clusters with open faces than in *closo*-heteroboranes.

It has also been shown in the studied architectures that the nature of bonding is reflected in the molecular observables such as the molecular electrostatic potential surface. Roughly speaking, where electron distribution is opposed to the classical electronegativity complex, such an electron distribution might

be attributed to multicenter bonding. On the other hand, the classical bonding indicates the classical electronegativity concept. Vector analyses of the experimental and computed dipole moments support such an observation.

Conflicts of interest

There are no conflicts to declare.

Acknowledgements

This work was supported by the research project RVO 61388963 of the Czech Academy of Sciences. We acknowledge the financial support from the Czech Science Foundation (17-08045S).

Notes and references

1 (*a*) W. N. Lipscomb, *Boron Hydrides*, Benjamin, New York, 1963; (*b*) more recent examples are outlined in D. Hnyk and D. A. Wann, Boron – the Fifth Element, in *Challenges and Advances in Computational Chemistry and Physics*, ed. D. Hnyk and M. McKee, Springer, Heidelberg, New York, Dordrecht and London, 2015, ch. 2, vol. 20; (*c*) the nature of a chemical bond is reflected in bond lengths, see P. Pykkö and M. Atsumi, *Chem. – Eur. J.*, 2009, **15**, 186–197.

2 R. C. Bochicchio, R. Ponec and F. Uhlík, *Inorg. Chem.*, 1997, **36**, 5363–5368.

3 R. M. Lobayan, R. C. Bochicchio, A. Torre and L. Lain, *J. Chem. Theory Comput.*, 2009, **5**, 2030–2043.

4 K. A. Lyssenko, M. Y. Antipin and V. N. Lebedev, *Inorg. Chem.*, 1998, **37**, 5834–5843.

5 K. Hedberg and V. Schomaker, *J. Am. Chem. Soc.*, 1951, **73**, 1482–1487.

6 H. Stammler, S. Blomeyer, R. J. F. Berger and N. W. Mitzel, *Angew. Chem., Int. Ed.*, 2015, **54**, 13816–13820.

7 Although PRDDO keeps a partially differential overlap and does not neglect it completely unlike CNDO, this approach is still empirically-based.

8 D. A. Dixon, D. A. Kleier, T. A. Halgren, J. H. Hall and W. N. Lipscomb, *J. Am. Chem. Soc.*, 1977, **99**, 6226–6237.

9 (*a*) P. Schleyer, G. Subramanian and A. Dransfeld, *J. Am. Chem. Soc.*, 1996, **118**, 9988–9989; (*b*) G. D. Graham, D. S. Marynick and W. N. Lipscomb, *J. Am. Chem. Soc.*, 1980, **102**, 2939–2945; (*c*) E. D. Jemmis, *J. Am. Chem. Soc.*, 1982, **104**, 7017–7020; (*d*) R. F. W. Bader and D. A. Legare, *Can. J. Chem.*, 1992, **70**, 657–676; (*e*) E. D. Jemmis, G. Subramanian, I. H. Srivastava and S. R. Gadre, *J. Phys. Chem.*, 1994, **98**, 6445–6451; (*f*) K. Takano, M. Izuho and H. Hosoya, *J. Phys. Chem.*, 1992, **96**, 6962–6969; (*g*) E. D. Jemmis and G. Subramanian, *J. Phys. Chem.*, 1994, **98**, 9222–9226; (*h*) Y. Sahin, C. Präsang, M. Hofmann, G. Geiseler, W. Massa and A. Berndt, *Angew. Chem.*, 2005, **117**, 1670–1673; (*i*) D. R. Armstrong, M. A. Fox and K. Wade, *J. Organomet. Chem.*, 2012, **721**, 130–136; (*j*) V. Dyczmons, M. Horn, P. Botschwina and A. Meller, *THEOCHEM*, 1998, **1**, 137–149; (*k*) R. M. Lobayan, R. C. Bochicchio, A. Torre and L. Lain, *J. Chem. Theory Comput.*, 2011, **7**, 979–987; (*l*) A. Torre, L. Lain, R. Bochicchio and R. Ponec, *J. Comput. Chem.*, 1999, **20**, 1085–1090.

10 (*a*) G. Knizia, *J. Chem. Theory Comput.*, 2013, **9**, 4834–4843; (*b*) G. Knizia and J. E. M. N. Klein, *Angew. Chem., Int. Ed.*, 2015, **54**, 5518–5522.

11 (*a*) E. Reed, R. B. Weinstock and F. Weinhold, *J. Chem. Phys.*, 1985, **83**, 735; (*b*) D. Yu Zubarev and A. Boldyrev, *Phys. Chem. Chem. Phys.*, 2008, **10**, 5207–5217. This work references other ''empirically-based'' bonding tools; (*c*) I. A. Popov and A. I. Boldyrev, Boron – the Fifth Element, in *Challenges and Advances in Computational Chemistry and Physics*, ed. D. Hnyk and M. McKee, Springer, Heidelberg, New York, Dordrecht and London, 2015, ch. 1, vol. 20.

12 S. H. Bauer, *J. Am. Chem. Soc.*, 1937, **59**, 1096–1103.

13 (*a*) I. B. Sivaeva, V. I. Bregadze and S. Sjöberg, *Collect. Czech. Chem. Commun.*, 2002, **67**, 679–727 and the references therein; (*b*) W. H. Knoth, H. C. Miller, J. C. Sauer, J. H. Balthis, Y. T. Chia and E. L. Muetterties, *Inorg. Chem.*, 1964, **3**, 159–167.

14 For the structure of $B_{11}H_{14}^-$ with three hydrogen bridges, see: J. Fritchie, *Inorg. Chem.*, 1967, **6**, 1199–1203.

15 M. Hofmann and P. Schleyer, *Inorg. Chem.*, 1998, **37**, 5557–5565.

16 J. W. Bausch, G. K. S. Prakash and R. E. Williams, *Inorg. Chem.*, 1992, **31**, 3763–3768; see also the references therein.

17 F. Schlüter and E. Bernhardt, *Inorg. Chem.*, 2011, **50**, 2580–2589.

18 T. Schaper and Wilhelm Preetz, *Inorg. Chem.*, 1998, **37**, 363–365.

19 D. J. Wales, Encyclopedia of Inorganic Chemistry, *Electronic Structure of Clusters*, Wiley, Berlin, 2006.

20 (*a*) D. Hnyk, *Polyhedron*, 1997, **16**, 603–606; (*b*) M. Bühl, J. Gauss, M. Hofmann and P. Schleyer, *J. Am. Chem. Soc.*, 1993, **115**, 12385–12390.

21 J. Pecyna, B. Ringstrand, S. Domagała, P. Kaszyński and K. Woźniak, *Inorg. Chem.*, 2014, **53**, 12617–12626.

22 A. R. Turner, H. E. Robertson, K. B. Borisenko, D. W. H. Rankin and M. A. Fox, *Dalton Trans.*, 2005, 1310–1318.

23 D. Hnyk, M. Bühl, P. Schleyer, H. V. Volden, S. Gundersen, J. Müller and P. Paetzold, *Inorg. Chem.*, 1993, **32**, 2442–2445.

24 R. McLellan, N. M. Boag, K. Dodds, D. Ellis, S. A. Macgregor, D. McKay, S. L. Masters, R. Noble-Eddy, N. P. Platt, D. W. H. Rankin, H. E. Robertson, G. M. Rosaira and A. J. Welch, *Dalton Trans.*, 2011, **40**, 7181–7192.

25 J. L. Little, J. G. Kester, J. C. Huffman and L. J. Todd, *Inorg. Chem.*, 1989, **28**, 1087–1091.

26 (*a*) D. Hnyk, E. Vajda, M. Bühl and P. R. Schleyer, *Inorg. Chem.*, 1992, **31**, 2464; (*b*) H. Møllendal, S. Samdal, J. Holub and D. Hnyk, *Inorg. Chem.*, 2003, **42**, 3043–3046.

27 Of the five possible isomers of *closo*-$CB_{10}H_{11}^-$, only *closo*-2-$CB_{10}H_{11}^-$ exists: W. H. Knoth, *J. Am. Chem. Soc.*, 1967, **89**, 1274–1275. This was also analyzed in P. R. Schleyer and K. Najafian, *Inorg. Chem.*, 1998, **37**, 3454–3470.

28 I. D. Mackie, H. E. Robertson, D. W. H. Rankin, M. A. Fox and J. M. Malget, *Inorg. Chem.*, 2004, **43**, 5387–5392.

29 B. Ringstranda, D. Batemana, R. K. Shoemaker and Z. Janoušek, *Collect. Czech. Chem. Commun.*, 2009, **74**, 419–431.
30 D. Hnyk, D. W. H. Rankin, H. E. Robertson, M. Hofmann, P. v. R. Schleyer and M. Bühl, *Inorg. Chem.*, 1994, **33**, 4781–4786.
31 P. M. Garrett, G. S. Ditta and M. F. Hawthorne, *Inorg. Chem.*, 1970, **9**, 947–1948.
32 J. Holub, T. Jelínek and Z. Janoušek, *Collect. Czech. Chem. Commun.*, 2002, **67**, 949–952.
33 L. Schneider, U. Englert and P. Paetzold, *Z. Anorg. Allg. Chem.*, 1994, **620**, 1191–1193.
34 J. Holub, M. Bakardjiev, B. Štíbr, D. Hnyk, O. L. Tok and B. Wrackmeyer, *Inorg. Chem.*, 2002, **41**, 2817–2819.
35 (*a*) D. Hnyk, D. A. Wann, J. Holub, S. Samdal and D. W. H. Rankin, *Dalton Trans.*, 2011, **40**, 5734–5737; (*b*) H. Møllendal, S. Samdal, J. Holub and D. Hnyk, *Inorg. Chem.*, 2002, **41**, 4574–4578; (*c*) J. MacCurtain, P. Brint and T. R. Spalding, *J. Chem. Soc., Dalton Trans.*, 1985, 2591–2594.
36 T. Jelínek, B. Štíbr, J. Holub, M. Bakardjiev, D. Hnyk, D. L. Ormsby, C. A. Kilner, M. Thornton-Pett, H. J. Schanz, B. Wrackmeyer and J. D. Kennedy, *Chem. Commun.*, 2001, 1756–1757.
37 B. M. Gimarc, B. Dai and J. J. Ott, *J. Comput. Chem.*, 1989, **10**, 14–16.
38 T. Jelínek, B. Štíbr, J. Plešek, J. D. Kennedy and M. Thornton-Pett, *J. Chem. Soc., Dalton Trans.*, 1995, 431–437.
39 B. M. Gimarc and J. J. Ott, *J. Am. Chem. Soc.*, 1987, **109**, 1388–1392.
40 G. B. Dunks and M. F. Hawthorne, *Inorg. Chem.*, 1968, **7**, 1038–1039.
41 B. Štíbr, O. L. Tok, W. Milius, M. Bakardjiev, J. Holub, D. Hnyk and B. Wrackmeyer, *Chem. – Eur. J.*, 2008, **14**, 6529–6533.
42 E. D. Jemmis, E. G. Jayasree and P. Parameswaran, *Chem. Soc. Rev.*, 2006, **35**, 157–168 and the references therein.
43 R. M. Minyaev, V. I. Minkin, T. N. Gribanova and A. G. Starikov, *Russ. Chem. Bull., Int. Ed.*, 2004, **53**, 1159–1167.
44 M. A. Fox, A. E. Goeta, A. K. Hughes and A. L. Johnson, *J. Chem. Soc., Dalton Trans.*, 2002, 2132–2141.
45 F. A. Kiani and M. Hofmann, *Inorg. Chem.*, 2004, **43**, 8561–8571.
46 M. A. Fox, A. E. Goeta, J. A. K. Howard, A. K. Hughes, A. L. Johnson, D. A. Keen, K. Wade and Ch. C. Wilson, *Inorg. Chem.*, 2001, **40**, 173–175.
47 D. Hnyk, M. Hofmann, P. Schleyer, M. Bühl and D. Rankin, *J. Phys. Chem.*, 1996, **100**, 3435–3440.
48 (*a*) J. Holub, T. Jelínek, D. Hnyk, Z. Plzák, I. Císařová, M. Bakardjiev and B. Štíbr, *Chem. – Eur. J.*, 2001, **7**, 1546–1554; (*b*) J. Holub, P. Melichar, Z. Růžičková, J. Vrána, D. A. Wann, J. Fanfrlík, D. Hnyk and A. Růžička, *Dalton Trans.*, 2017, **46**, 13714–13719.
49 M. Bakardjiev, J. Holub, B. Štíbr, D. Hnyk and B. Wrackmeyer, *Inorg. Chem.*, 2005, **44**, 5826–5832.
50 J. Plešek, B. Štíbr, D. Hnyk, T. Jelínek, S. Heřmánek, J. D. Kennedy, M. Hofmann and P. R. Schleyer, *Inorg. Chem.*, 1998, **37**, 3902–3909.
51 D. Hnyk, J. Holub, S. A. Hayes, M. F. Robinson, D. A. Wann, H. E. Robertson and D. W. H. Rankin, *Inorg. Chem.*, 2006, **45**, 8442–8446.
52 D. Hnyk, M. Hofmann and P. R. Schleyer, *Collect. Czech. Chem. Commun.*, 1999, **64**, 993–1000.
53 M. G. S. Londesborough, Z. Janoušek, B. Štíbr, D. Hnyk, J. Plešek and I. Císařová, *Dalton Trans.*, 2007, 1221–1228.
54 J. P. F. Nunes, J. Holub, D. W. H. Rankin, D. A. Wann and D. Hnyk, *Dalton Trans.*, 2015, **44**, 11819–11826.
55 TURBOMOLE Version 6.6, 2014, a development of University of Karlsruhe and Forschungszentrum Karlsruhe GmbH, 1989–2007, TURBOMOLE GmbH, since 2007.
56 M. J. Frisch, G. W. Trucks, H. B. Schlegel, G. E. Scuseria, M. A. Robb, J. R. Cheeseman, G. Scalmani, V. Barone, G. A. Petersson, H. Nakatsuji, X. Li, M. Caricato, A. Marenich, J. Bloino, B. G. Janesko, R. Gomperts, B. Mennucci, H. P. Hratchian, J. V. Ortiz, A. F. Izmaylov, J. L. Sonnenberg, D. Williams-Young, F. Ding, F. Lipparini, F. Egidi, J. Goings, B. Peng, A. Petrone, T. Henderson, D. Ranasinghe, V. G. Zakrzewski, J. Gao, N. Rega, G. Zheng, W. Liang, M. Hada, M. Ehara, K. Toyota, R. Fukuda, J. Hasegawa, M. Ishida, T. Nakajima, Y. Honda, O. Kitao, H. Nakai, T. Vreven, K. Throssell, J. A. Montgomery Jr., J. E. Peralta, F. Ogliaro, M. Bearpark, J. J. Heyd, E. Brothers, K. N. Kudin, V. N. Staroverov, T. Keith, R. Kobayashi, J. Normand, K. Raghavachari, A. Rendell, J. C. Burant, S. S. Iyengar, J. Tomasi, M. Cossi, J. M. Millam, M. Klene, C. Adamo, R. Cammi, J. W. Ochterski, R. L. Martin, K. Morokuma, O. Farkas, J. B. Foresman and D. J. Fox, *Gaussian 09, Revision A.02*, Gaussian, Inc., Wallingford CT, 2016.
57 (*a*) P. Flükiger, H. P. Lüthi, S. Portmann and J. Weber, *MOLEKEL 4.3*, Swiss Center for Scientific Computing, Manno (Switzerland), 2000; (*b*) S. Portmann and H. P. Lüthi. *MOLEKEL: CHIMIA*, 2007, vol. 28, 555.
58 J. Fanfrlík, A. Pecina, J. Řezáč, R. Sedlak, D. Hnyk, M. Lepšík and P. Hobza, *Phys. Chem. Chem. Phys.*, 2017, **19**, 18194–18200.
59 J. S. Miller and J. J. Novoa, *Acc. Chem. Res.*, 2007, **40**, 189–196.
60 H. Jacobsen, *Dalton Trans.*, 2009, 4252–4258.
61 M. L. McKee, M. Bühl, O. P. Charkin and P. R. Schleyer, *Inorg. Chem.*, 1993, **32**, 4549–4554.
62 J. E. D. Bene, I. Alkorta and J. Elguero, *J. Phys. Chem. A*, 2016, **120**, 5745–5751.
63 J. Fanfrlik and D. Hnyk, *CrystEngComm*, 2016, **18**, 8982–8987.
64 J. Fanfrlík, A. Přáda, Z. Padělková, A. Pecina, J. Macháček, M. Lepšík, J. Holub, A. Růžička, D. Hnyk and P. Hobza, *Angew. Chem., Int. Ed.*, 2014, **53**, 10139–10142.
65 D. Hnyk, V. Všetečka, L. Drož and O. Exner, *Collect. Czech. Chem. Commun.*, 2001, **66**, 1375–1379.
66 W. N. Lipscomb, in *Boron Hydride Chemistry*, ed. E. L. Muetterties, Academic Press, New York, 1975.
67 A. Pecina, M. Lepsik, D. Hnyk, P. Hobza and J. Fanfrlík, *J. Phys. Chem. A*, 2015, **119**, 1388–1395.
68 T. Kar and K. Jug, *Int. J. Quantum Chem.*, 1995, **53**, 407–412.